



**DESIGN, ANTIOXIDANT EVALUATION AND MOLECULAR DOCKING  
STUDY OF HETEROCYCLIC SCHIFF BASES AS POTENTIAL ANTICANCER  
AGENTS**

**Cordelia U. Dueke-Eze<sup>1\*</sup>, Ifeoma Orabueze<sup>2</sup> and Inemesit A. Udofia<sup>3</sup>**

<sup>1</sup>*Department of Chemistry, University of Lagos, Lagos State, Nigeria*

<sup>2</sup>*Department of Pharmacognosy, College of Medicine, University of Lagos, Lagos state, Nigeria.*

<sup>3</sup>*Department of Chemistry, Covenant University, Ogun State, Nigeria.*

*\*Corresponding author: cdueke-eze@unilag.edu.ng, +2348037134202*

---

**Abstract**

The growing scientific interest in oxidative stress and antioxidants stems from their well-established role in mitigating free radical-induced cellular and tissue damage. Three Schiff bases derived from isonicotinic acid hydrazide and furan-2-carboxaldehyde (INH-Furan), pyrrole-2-carboxaldehyde (INH-Pyrrole), thiophene-2-carboxaldehyde (INH-Thio) have been synthesized and characterized by FTIR, NMR and elemental analysis. The Antioxidant potential were evaluated using DPPH, FRAP, Nitric oxide radical scavenging and Total Antioxidant Capacity assays with ascorbic acid as reference. The compounds exhibited concentration-dependent activities, showing strong radical scavenging effects. IC<sub>50</sub> values ranked their activity as ascorbic acid > INH-Pyrrole > INH-Furan > INH-Thio. Molecular docking against EGFR wild type and resistant mutants revealed favorable binding energies supported by hydrogen bonding, Pi-Pi stacking, and salt bridge interactions. These findings show that the Schiff bases are promising scaffolds for developing potent antioxidants and EGFR inhibitors that can withstand drug resistance.

**Keywords:** Schiff base, antioxidant activity, free radicals, scavenging, molecular docking

## 1.0 Introduction

Human life activities are strongly tied to free radicals, which are in charge of supplying vitality to the cells, organs, and tissues [1]. Free radicals are continuously created and scavenged by the human anatomy to sustain active stability. Free radicals can protect the body from diseases like bacteria and fungi when it is in good health. Under normal conditions, free radicals can shield the body from infections like fungus and bacteria. However, when it is unbalanced, excessive free radicals damage cells, causing early aging [2], HIV [3], renal disease [4], pregnancy [5], cancer [6], and cataract [7]. It is very important that the right levels of natural antioxidants including glutathione, vitamin C, and vitamin E are maintained by the biological system to avoid major health issues,

Antioxidants are chemicals that may work together with free radicals and safeguard cells from oxidative damage. They come in both natural and synthetic forms. Strong antioxidant qualities have been demonstrated in a variety of compounds, however,

understanding of antioxidant mechanism and the development of more effective and harmless antioxidants remain a great challenge.

Schiff bases represent a significant class of chemical compounds as investigational tool. They are compounds that have an azomethine group (-C=N-) and obtained by the condensation of an amine and a carbonyl [8-9]. Their substantial biological activities, such as antioxidant [10-16], antibacterial [13], antifungal [17], antiviral [18], anticancer [16, 19], antitumor [20, 21] and anti-inflammatory [22] have drawn a lot of attention in the medical and pharmaceutical families. Simple synthetic techniques can be used to add potentially active moiety to the Schiff base skeletons. Schiff bases have high radical scavenging action [23, 24]. Also, the transmission of stimulus via the transduction pathway due to the binding of epidermal growth factor (EGF) to EGF receptor (EGFR) on the cell surface can regulate the cell proliferation, differentiation, and migration [25].

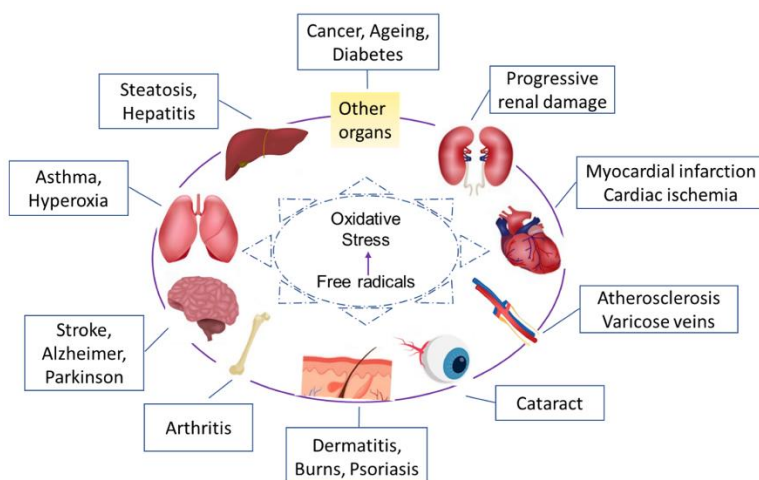


**Figure 1:** Most common oxidative stress related diseases [1]

The EGFR family plays a critical role in vital cellular processes and in various cancers and is a proven target in the treatment of cancer [26, 27]. Some EGFR kinase inhibitors are available for use such as efitinib, erlotinib, lapatinib, and TAK-285 [28]. These inhibitors are not only effective against the wild-type EGFR but also the mutant-type [29, 25]. Clinically, the efficacy of these kinase inhibitors is often of limited duration due to the kinase resistance to these drugs. This resistance is as a result of the substitution of threonine 790 with methionine (T790M). Threonine 790 is often referred to as the gatekeeper residue in the EGFR protein because of its strategic location at the entrance to a hydrophobic pocket in the back of the ATP binding cleft, hence substitution of this residue with methionine is believed to cause resistance by steric interference with the binding kinase inhibitors [30, 31].

Besides targeting T790M inhibition, some irreversible inhibitors have been developed to target CYS797, which is located at the entrance to the adenosine triphosphate binding cleft (28, 32). Their mode of binding is via covalent bonding interaction with the CYS797. Concerns have been raised about their selectivity with respect to kinases due to their reactivity with other cysteine residues [25, 29, 33]. It is there important to look for more potent, noncovalent, irreversible inhibitors against both the wild and T790M/L858R double-mutated EGFR. Our team is interested in the use Schiff base molecule to study the properties of antioxidants using nitric oxide radicals, DPPH radicals, Ferric reducing antioxidant Power and total antioxidant assay and as inhibitors for the EGFR double mutant.

## 2.0 Materials and Methods

### Materials

Aldrich Chemical Ltd. provided all of the chemicals and solvents that were available for purchase. They are employed without additional purification and are of spectroscopic or analytical quality. Melting points are uncorrected and were calculated using a Stuart SMP3 melting point equipment. On a Digilab Win-IR Pro ATR spectrometer of the FTS 7000 series, infrared spectra were captured as particles using a diamond ATR (attenuated total reflectance) accessory by applying the thin-film technique. DMSO-d<sub>6</sub> solution was used to record the <sup>1</sup>H and <sup>13</sup>C NMR spectra, which are referred to the solvent peaks using a Varian 300 MHz spectrometer. The Perkin-Elmer 2400 CHNS/O analyzer was used to perform elemental studies. Ascorbic acid (99%), trichloroacetic acid (TCA), hydrogen peroxide, potassium ferricyanide, iron(II) chloride, methanol, 3-(2-pyridyl)-5,6-diphenyl-1,2,4-triazine-4',4''-disulfonic acid sodium salt (ferrozine), iron(III) chloride, and hydrochloric acid (Germany).

### 2.1 Synthesis of Schiff bases

An ethanol (10 mL) solution of isonicotinic acid hydrazide (10 mmol.) was mixed with a solution of the corresponding aldehyde furan-2-carboxaldehyde (INH-Furan), (pyrrole-2-carboxaldehyde (INH-Pyrrole), or thiophene-2-carboxaldehyde (INH-Thio) (10 mmol.) in ethanol (10 mL). At 60°C, the reaction mixture was stirred for 8 h with the addition of glacial acetic acid (0.3 mL) after which it was left to cool to room temperature. Filtration was used to collect and

recrystallize the resultant precipitate from ethanol.

## 2.2 Evaluation of antioxidant activities

### DPPH radical scavenging assay

A decrease in the absorbance of DPPH was used to quantify the synthetic compounds' capacity to scavenge free radicals according to the methods of [34] and [35] with some modifications. The serial solutions of the samples (25– 100 µg/mL) were prepared using distilled water. Then 4 mL of each solution was added to 1 mL of methanolic solution of DPPH (0.01 mM). The resulting mixture was thoroughly shaken and allowed to stand for 30 min in a dark closet. Absorbance was spectrophotometrically measured at 517 nm. Methanol was used as the blank and ascorbic acid was used for the standard (serial diluted solutions of ascorbic acids). All assays were done in triplicates. The scavenging effect of the samples were presented as percentage inhibition.

Scavenging Effect (%) =  $(D_0 - D_1)/D_0 \times 100$   
Where  $D_0$  represents the absorbance of the control and  $D_1$  the absorbance in the presence of the sample of extract and standard.

### 2.3 Nitric oxide scavenging activity

Using spectrophotometry, the nitric oxide scavenging activity was determined as reported by [36] with some modification. Aqueous sodium nitroprusside at physiological pH has been documented to produce nitrite ions [37]. This it does by generating nitric oxide which interacts with oxygen to produce the nitrite ions. Phosphate buffered saline of pH 7.4 was prepared with sodium nitroprusside (5 mM L<sup>-1</sup>). The serial dilute solutions of the samples (25– 100

µg/mL) were made. The buffer was mixed with 50 µL of each of the solutions of the samples. The mixture was incubated at 25°C for 30 min. Then 1.5 mL of the incubated mixture was diluted with 1.5 mL of Griess reagent (1% sulphanilamide, 2% phosphoric acid and 0.1% N-1- naphthylethylenediamine dihydrochloride). Absorbance was taken at 546 nm. Ascorbic acid was used as the positive standard, while 10 mM sodium nitroprusside and phosphate buffered saline were used as the negative control.

### 2.4 Ferric reducing antioxidant Power (FRAP)

The reducing power of samples were determined using the modified method of [39]. An aliquot of the samples (1.0 mL) at various serially diluted concentrations (25, 50, 75 and 100 µg/mL) were mixed with phosphate buffer (2.5 mL, 0.2M, pH (6.6) and potassium ferricyanide [K<sub>3</sub>Fe(CN)<sub>6</sub>] (2.5 mL, 1%). The mixtures were incubated at 50 °C for 20 min. Trichloroacetic acid (10%, 2.5 mL) was added to each of the mixture and centrifuge at 1000 rpm for 15 min. A volume of 2.5 mL of each of the resulting supernatants was mixed with 0.1% of freshly prepared iron (III) chloride (0.5 mL) and distilled water (2.5 mL). Absorbance was measured at 700 nm using methanol as the blank. An increasing absorbance value is an indication of the reducing power of the samples/substance. The reference drug used for the study was ascorbic acid (vitamin C), also serially prepared. Each of the experiments was done in triplicate.

## 2.5 Total antioxidant capacity (TAC)

The total antioxidant capacity of the samples was determined using modified [40]. Each of the samples were diluted serially (25, 50, 75 and 100 ug/mL) using ethanol/methanol. An aliquot (0.4 mL) of the solution of the diluted sample was mixed within a vial containing 4 mL of a reagent solution (0.6 M sulfuric acid, 4 mM ammonium molybdate, and 28 mM sodium phosphate). A water bath was used to incubate the vial at the temperature of 95 °C for 90 min. The absorbance was taken at 695 nm against ethanol/methanol as blank after the vial has been cooled to room temperature. Assays of all the serially diluted solutions of the samples were run in triplicate.

## 2.6 Molecular Docking Protocol

Flexible ligand with a rigid receptor docking simulation was performed using Autodock

Final Internal Energy (van der Waals + Hydrogen bond + desolvation Energy) + ( Final Total Internal Energy) + ( Torsional Free Energy) – (Unbound systems's Energy

Prior to the molecular docking simulations, the molecular geometries of the inhibitors were optimization the B3LYP/ 6-311+G(2d,p) density functional of theory (DFT) method and the stability of the ligands were checked by means of frequency calculations, that they had no imaginary frequency. The reason for performing the geometry optimization was to ensure that the molecular structures used were geometrically stable structures. The DFT calculations were done with the help of Gaussian 16 suites of programs, provided by means of computational resource on SEAGrid [43]. The interaction pictures were generated with

4.2.6 [41]. The choice of Autodock 4.2.6 was borne out of the knowledge of its better performance than Autodock vina in terms of reproducing experimental binding energy values [42]. Knowledge of the active sites of the protein were obtained from previously published articles with similar proteins [25]. Conformational space of the complex was sampled using the Lamarckian Genetic Algorithm. The number of evaluations was 2500000, 100 runs were performed and the rest of the docking parameters were set to default. The conformation with the lowest free energy of binding for each of the ligands and the corresponding protein structure was chosen as the best inhibitor for the protein. Autodock 4.2.6 presents the free energy of binding as:

the help of UCSF Chimera, alpha version 1.17 (build 42434) [44] and Discovery Studio Visualizer v24.1.0.23298.

## 3.0 Results and discussion

### Synthesized Schiff bases

INH-Pyrrole, INH-Furan and INH-Thio are heterocyclic Schiff bases that were produced by condensation of INH with Pyrrole-2-carboxaldehyde, furan-2-carboxaldehyde, and thiophene-2-carboxaldehyde in reasonable yields (Scheme 1). The compounds were purified from ethanol.

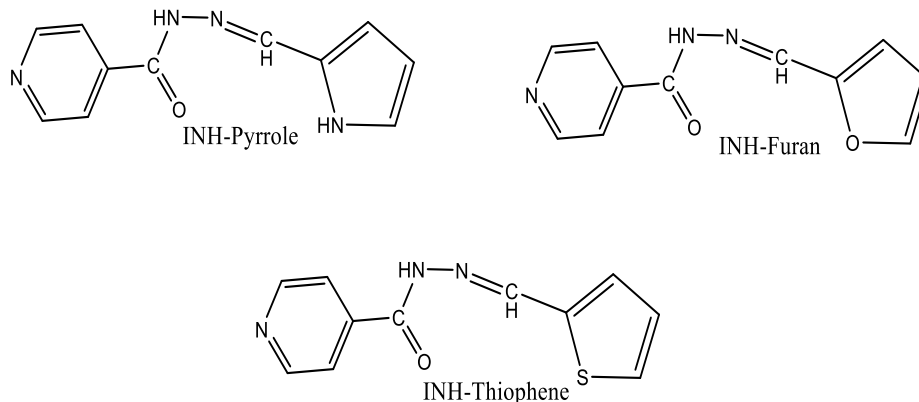


**Figure 2:** Structure of the synthesized Schiff bases [45]

**Tables 1 and 2** afford a summary of the compounds' analytical and spectroscopic data.

**Table 1:** Physical and Analytical data of Schiff bases

Sample	Molecular weight (g/mol)	Mpt °C	% yield	Microanalysis Calculated(Found)		
				C	H	N
INH-Furan	C <sub>11</sub> H <sub>9</sub> N <sub>3</sub> O <sub>2</sub>	223-225	40	61.39(61.23)	4.22(4.07)	19.53(19.99)
INH-Pyrrole	C <sub>11</sub> H <sub>10</sub> N <sub>4</sub> O	234-236	87	61.67(62.16)	4.71(4.64)	26.15(26.27)
INH-Thio	C <sub>11</sub> H <sub>9</sub> N <sub>3</sub> OS	241-242	81	57.13(57.64)	3.92(3.85)	18.17(18.93)

**Table 2:** Characteristics IR and NMR bands of Schiff bases

Sample	IR Bands (cm <sup>-1</sup> )			Chemical shift δ(ppm)	
	νNH	νC=O	νC=N	HC=N	δC
				δH	
INH-Furan	-	1644	1617	8.35	140.89
INH-Pyrrole	3056	1645	1594	8.29	141.48
INH-Thio	3028	1661	1593	8.68	140.94

The presence of a band in the IR spectra in the range of 1593–1617 cm<sup>-1</sup> and a singlet at 8.29–8.68 ppm in the compounds' proton NMR spectra certified the compounds' formation. The elemental analysis supports the composition of the compounds.

### 3.1 Antioxidant assay

The antioxidant power in DPPH assay, nitric oxide scavenging activity, ferric reducing antioxidant power and total antioxidant capacity methods were used to evaluate the antioxidant effects of the synthesized test antioxidants.

### 3.2 The DPPH test

The concentration response curve for the radical scavenging effect of the reference positive control (ascorbic acid) and the test synthetic antioxidant samples (1NH-Furan, 1NH-Pyrrole and 1NH-Thio) is displayed in

Figures 3-5. Both the synthetic antioxidants and ascorbic acid (reference positive control), had concentration-dependent radical scavenging activities.

**Table 3: DPPH Scavenging Activity (% Inhibition)**

	µg/mL			
	25	50	75	100
1NH-Furan	42.515 ± 0.219	54.425 ± 0.629	74.210 ± 0.425	80.145 ± 0.007
1NH-Pyrrole	42.705 ± 0.049	55.475 ± 0.219	72.830 ± 0.000	78.495 ± 0.006
1NH-Thio	35.670 ± 0.028	42.705 ± 0.077	54.525 ± 0.205*	68.220 ± 0.141*
A. ACID	45.670 ± 0.028	64.705 ± 0.077	85.375 ± 0.007	98.220 ± 0.141

The DPPH inhibition (%) of the standard reference, the ascorbic acid was 98.200% at 100 µg/mL

while the next highest percentage inhibition was INH-Furan (80.145%). High percentage inhibition number indicates strong scavenging activity, meaning that a higher amount of DPPH radical has been reduced by an antioxidant and good activity [46]. The IC<sub>50</sub> values of ascorbic acid and INH-Furan were 1.1825 and 1.5334 µg/mL, respectively (Figures 4 and 5). DPPH undergoes a reduction reaction when it comes in contact with a hydrogen atom donating agent/compound. This is the parameter that was measured and calculated to percentage inhibition. The IC<sub>50</sub> values of INH-Furan, INH-Pyrrole, INH-Thio and ascorbic acid were 1.5334, 1.5077, 2.4744, and 1.1825 respectively. The interpretation of the IC<sub>50</sub> as recorded in the study (Figure 5) showed that a lower (significant, p < 0.05) concentration of ascorbic acid was needed to affect free radical neutralization reaction compared to test antioxidant samples. DPPH\* is a stable

free radical which when in contact with antioxidant readily accept an electron or H\* to be reduced to DPPH<sub>2</sub>. The degree of colour change from the characteristic purple colour of radical DPPH to light yellow colour of the mixture is an indication of antioxidant activity and what is measured [47, 48].

The result of the DPPH study indicates that the radical-quenching potential of INH-Furan, INH-Pyrrole may be comparable to the reference antioxidant, ascorbic acid (Table 3). While a larger amount of INH-Thio is needed to achieve 50% of the scavenging effect (IC<sub>50</sub>) compared to other test antioxidant samples and the reference drug, ascorbic acid.

A high DPPH value is an indication of strong antioxidant activity. Thus, the ascorbic acid, followed by the 1NH-Furan and then the 1NH-Pyrrole based on the obtained results suggest they have effective scavenging effect of free radicals while 1NH-Thio at 68.220% may be classified to be moderate and less active as an antioxidant compared to other analytes. They all possibly have the potential

health application in relation to protecting against oxidative stress and related diseases. The difference observed at the individual's

ability to do so may be as a result of the molecular structure.

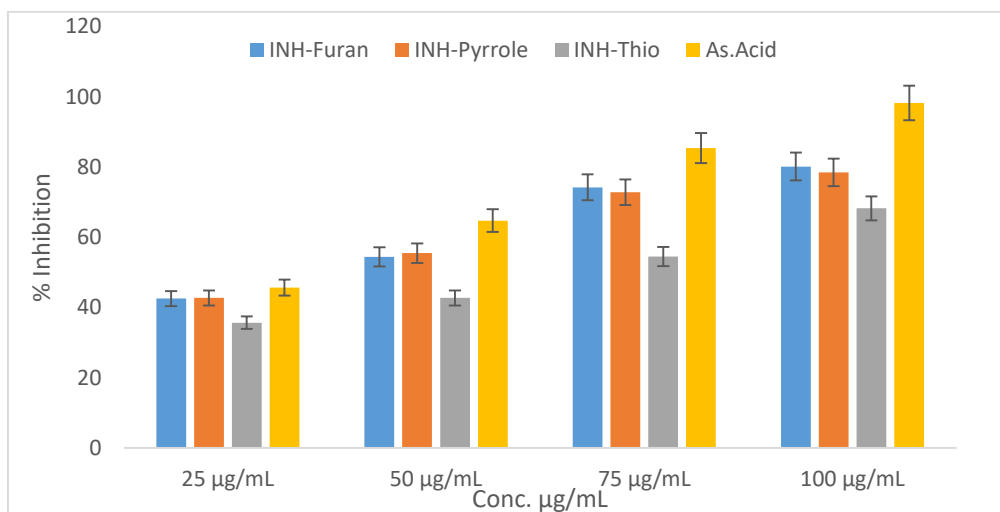


**Figure 3:** Comparative DPPH free radical scavenging effect of INH-Furan, INH-Pyrrole, INH-Thio and ascorbic acid; Values are mean ± SEM, n = 3

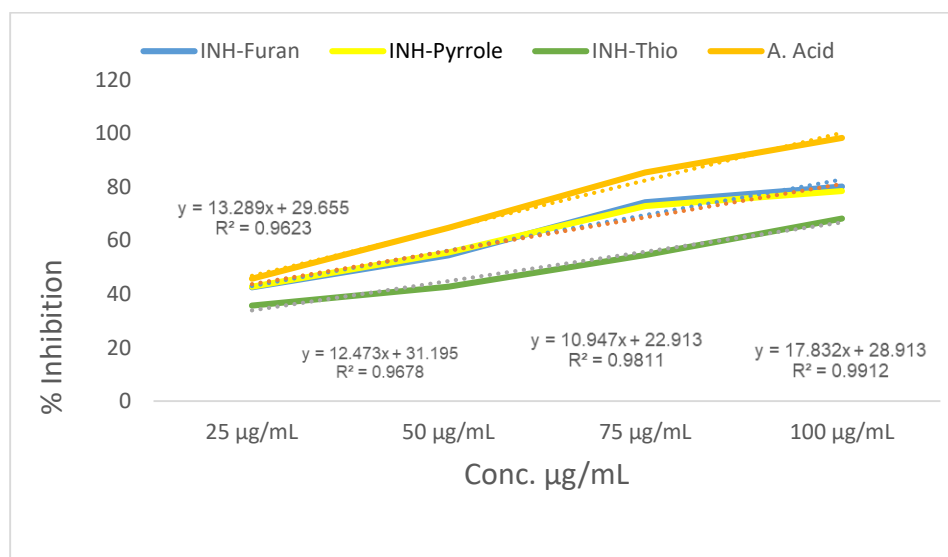


**Figure 4:** Line graph representation of the Percentage DPPH free radical scavenging effect of: A: INH-Furan, INH-Pyrrole, INH-Thio and ascorbic acid; Values are mean ± SEM, n = 3;

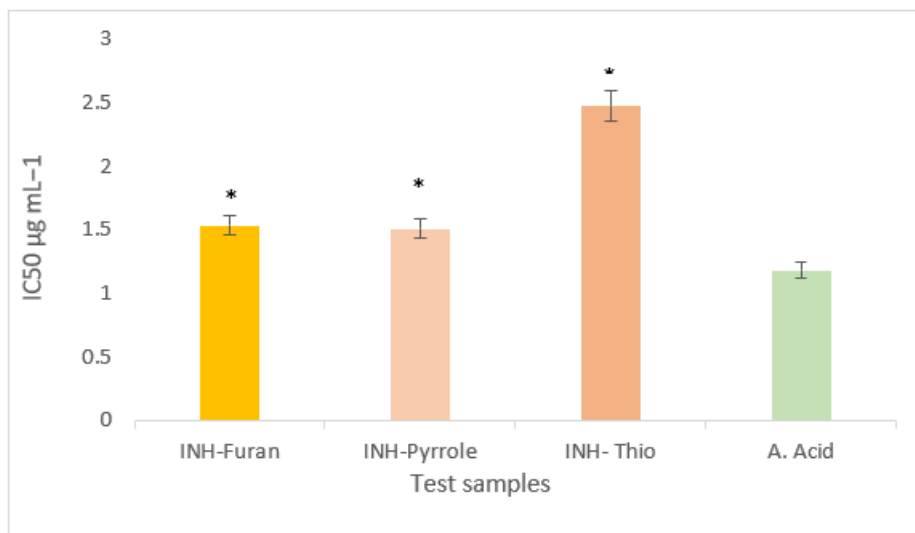


**Figure 5:** IC<sub>50</sub> of the free radical scavenging effects of test samples (INH-Furan, INH-Pyrrole, INH-Thio) and Ascorbic Acid; n= 3; Significantly different at \*p < 0.05 compared with IC<sub>50</sub> of the ascorbic acid; IC<sub>50</sub> of INH-Furan, INH-Pyrrole, INH-Thio and Ascorbic Acid: 1.5334, 1.5077, 2.4744, and 1.1825 respectively; R<sup>2</sup>: 0.9644, 0.9678, 0.9811 and 0.9912.

### 3.3 Ferric reducing potential antioxidant scavenging activity (Absorbance)

Table 4 shows the absorbance of the synthesized test samples (INH-Furan, INH-Pyrrole, INH-Thio) and the ascorbic acid after performing the FRAP activity at various concentrations. Their absorbance values were concentration-dependent. Absorbance increased with increased concentration of the analytes. Thus, indicating their increased ability to donate more electrons to Fe<sup>3+</sup> and effect the reduction of Fe<sup>3+</sup> to Fe<sup>2+</sup>, their increased ability to reduce oxidized species. Figures 6, 7 and 8 show the pictorial representation of the FRAP activities of the test samples compared to ascorbic acid and

their IC<sub>50</sub>. The FRAP assay results demonstrated that all the test samples exhibited strong reducing potential at increased concentrations (50 - 100 µg/mL) compared to the low concentration (25 µg/mL). However, the reference drug, ascorbic acid has a stronger reducing power potential (Figure 7, 8) compared to the test samples which is statistically different (p<0.05). The reducing power activities of INH-Furan, INH-Pyrrole, INH-Thio showed no statistical difference among themselves and across the different concentrations (Table 4, Figures 6 -8).

**Table 4: Ferric Reducing Antioxidant Power**

	µg/mL			
	25	50	75	100
1NH-Furan	0.037 ± 0.001	0.157 ± 0.001	0.2345 ± 0.001*	0.377 ± 0.001*
1NH-Pyrrole	0.038 ± 0.001	0.155 ± 0.001	0.241 ± 0.009*	0.379 ± 0.001*
1NH-Thio	0.032 ± 0.000	0.154 ± 0.000	0.233 ± 0.001*	0.366 ± 0.017*
A. ACID	0.159 ± 0.001	0.214 ± 0.000	0.443 ± 0.000	0.512 ± 0.000

Values are mean ± SEM, n = 3; significantly different at \*p < 0.05 compared to ascorbic acid

The reducing power activities of INH-Furan, INH-Pyrrole, INH-Thio showed no statistical difference among themselves and across the different concentrations (Table 4, Figures 6 - 8). High concentrations of the test samples are needed to induce strong reducing or electron donating effects as a mechanism of antioxidant activity compared to the standard. For example, ascorbic acid showed

greater antioxidant potential than the test INH-Furan. INH-Furan at 100 µg/mL caused reduction of Fe<sup>3+</sup> complex to Fe<sup>2+</sup> absorbance of 0.377 ± 0.001 compared to ascorbic acid value of 0.512 ± 0.000. The higher the absorbance value the stronger its reduction capacity, electron donating power, the better an antioxidant potential [47, 49]. In relation to FRAP antioxidant evaluation activity, ascorbic acid is significantly stronger than the test samples (Table 4; Figures, 6-7).

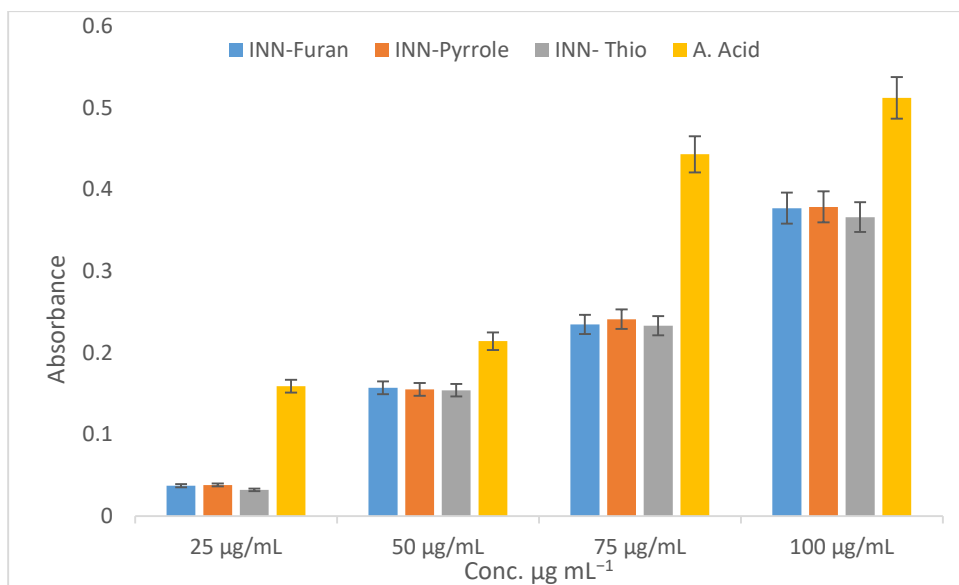


**Figure 6:** Comparative Reductive effect of INH-Furan, INH-Pyrrole, INH-Thio and ascorbic acid; Values are mean ± SEM, n = 3

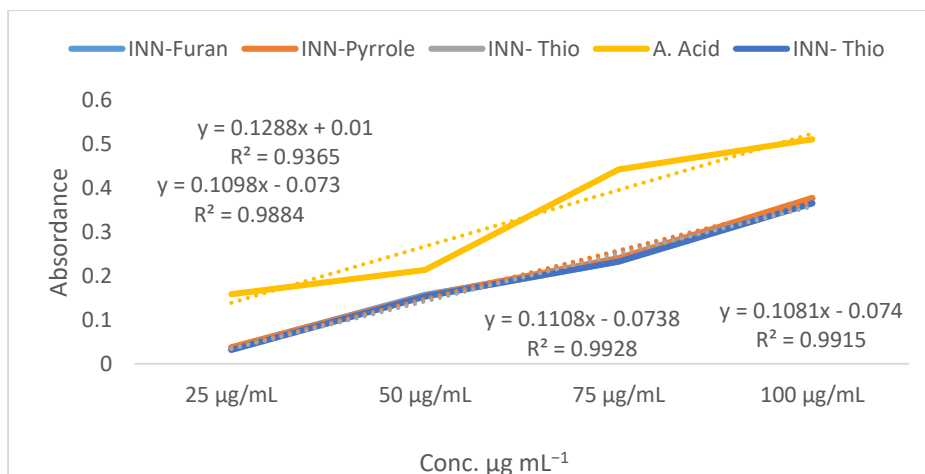


**Figure 7:** Line graph representation of Reductive effect of INN-Furan, INN-Pyrrole, INN-Thio and ascorbic acid; Values are mean  $\pm$  SEM, n = 3

The  $IC_{50}$  value of INN-Furan, INN-Pyrrole, INN-Thio and ascorbic acid were 456.0382, 451.929, 463.219, and 388.276  $\mu\text{g mL}^{-1}$  respectively. Thus, the order of reducing effect was ascorbic acid > INN-Pyrrole > INN-Furan > INN-Thio (Figures 7 and 8).

This reflects what was observed in DPPH scavenging effect  $IC_{50}$  (Figure 5). Compounds with effective reducing power may offer protective effects against oxidative-stress-mediated cellular damage.

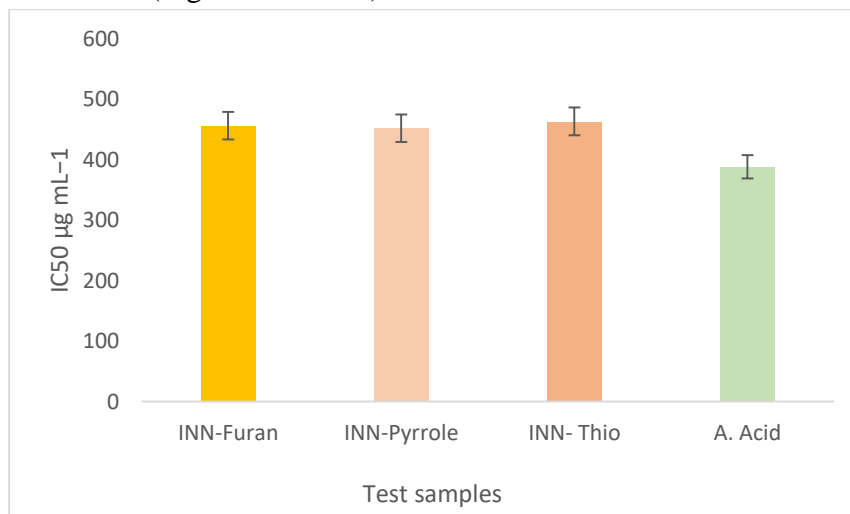


**Figure 8:**  $IC_{50}$  of the reducing effects of test samples (INN-Furan, INN-Pyrrole, INN-Thio) and Ascorbic Acid; n= 3; Significantly different at  $*p < 0.05$  compared with  $IC_{50}$  of the ascorbic acid;  $IC_{50}$  of INN-Furan, INN-Pyrrole, INN-Thio and Ascorbic Acid: 1456.038, 451.929, 463.219, and 388.276  $\mu\text{g mL}^{-1}$  respectively;  $R^2$ : 0.9884, 0.9928, 0.9915, and 0.9365

### 3.4 Nitric oxide scavenging radical (%Inhibition)

Nitric oxide scavenging assay is a different radical from DPPH\* and its assay is used to

measure the ability of an antioxidant to scavenge  $NO^*$  or its derivative [50]. It is a different method or pathway for measuring the antioxidant power of an agent. Thus,

scavenging nitric oxide radical (NO\*) profile of a test compound could be used to evaluate its oxidative stress reduction capability, and prevention of reactive nitrogen species RNS. Test sample(s) with good NO\* scavenging

effect suggest strong anti-inflammatory, vascular function protector and disease. Results are shown in Table 5 and Figures 9-11.

**Table 5: Nitric Oxide Scavenging Activity (% Inhibition)**

	µg/mL			
	25	50	75	100
1NH-Furan	30.28 ± 0.070	48.24± 0.000	60.29± 0.042*	62.57± 0.014*
1NH-Pyrrole	36.365 ± 0.007	52.345 ± 0.021	62.48 ± 0.000*	68.845 ± 0.007*
1NH-Thio	28.565 ± 0.007	38.43 ± 0.014	60.40 ± 0.028*	63.545 ± 0.007*
A. Acid	38.77 ± 0.014	58.93 ± 0.070	80.71 ± 0.255	90.695 ± 0.219

Values are mean ± SEM, n = 3; significantly different at \*p < 0.05 compared to ascorbic acid

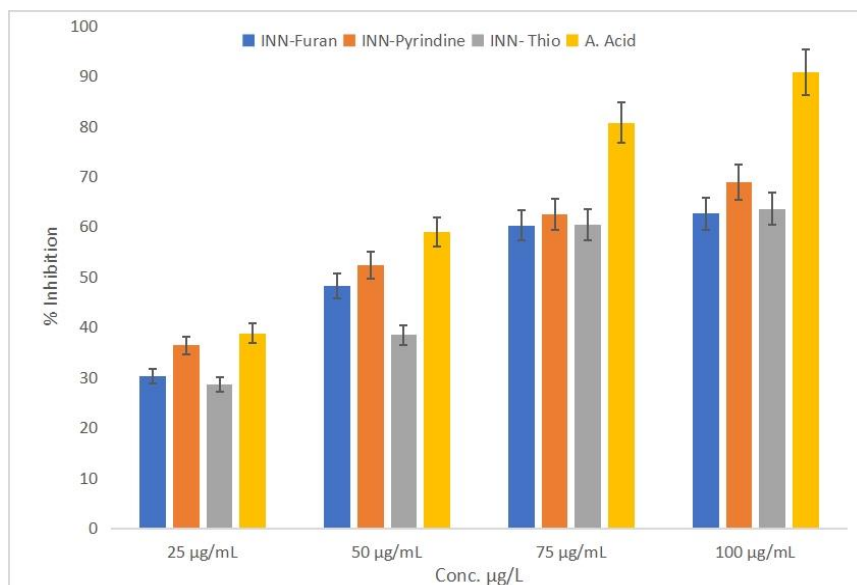


**Figure 9:** Comparative Percentage Nitric oxide scavenging activity of INH-Furan, INH-Pyrrole, INH-Thio and ascorbic acid; Values are mean ± SEM, n = 3

The percentage of inhibition showed that ascorbic acid (reference drug) is a significantly (p < 0.05) stronger antioxidant than all the test samples. This was also observed in their IC<sub>50</sub> presentation (Figure

11). The IC<sub>50</sub> of all the analytes showed antioxidant profile in relation to their ability to scavenge NO\* in the following order, ascorbic acid (1.527) > INH-Pyrrole (2.034) > INH-Furan (2.468) > INH-Thio (2.679). A

low IC<sub>50</sub> value indicates strong antioxidant effects.

no significant difference among them in their ability to scavenge NO\*.

Comparing the percentage of inhibition among the test samples showed that there was

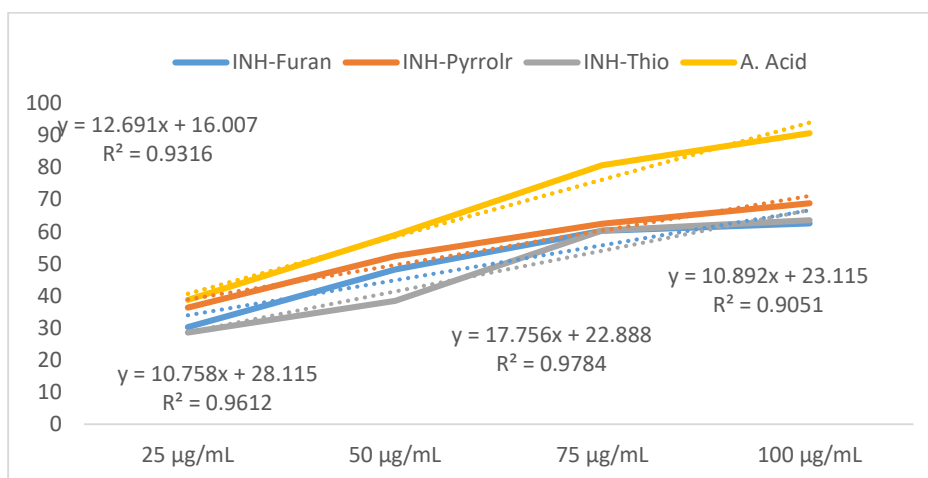


**Figure 10:** Line graph representation of Percentage Nitric oxide scavenging activity effect of INH-Furan, INH-Pyrrole, INH-Thio and ascorbic acid; Values are mean ± SEM, n = 3;

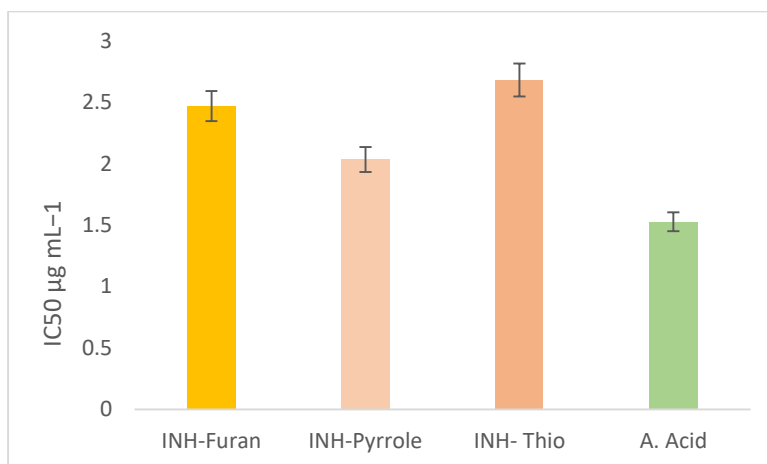


**Figure 11:** IC<sub>50</sub> of the Nitric oxide scavenging of test samples (INH-Furan, INH-Pyrrole, INH-Thio) and Ascorbic Acid; n = 3; Significantly different at \*p < 0.05 compared with IC<sub>50</sub> of the ascorbic acid; IC<sub>50</sub> of INH-Furan, INH-Pyrrole, INH-Thio and Ascorbic Acid: 2.468, 2.034, 2.679, and 1.527 µg mL<sup>-1</sup> respectively; R<sup>2</sup>: 0.9051, 0.9612, 0.9316, and 0.9784.

### 3.5 Total antioxidant capacity

The total antioxidant capacity (TAC) indicates the overall antioxidant ability of the analytes (test samples and the reference, ascorbic acid) [51]. Other assays discussed

above are specific mechanisms that contribute to the result of TAC. The TAC result (Figure 12) reflects the results gotten from DPPH, FRAP and NO assays. It follows

the same pattern or order of ascorbic acid > INH-Pyrrole > INH-Furan > INH-Thio.

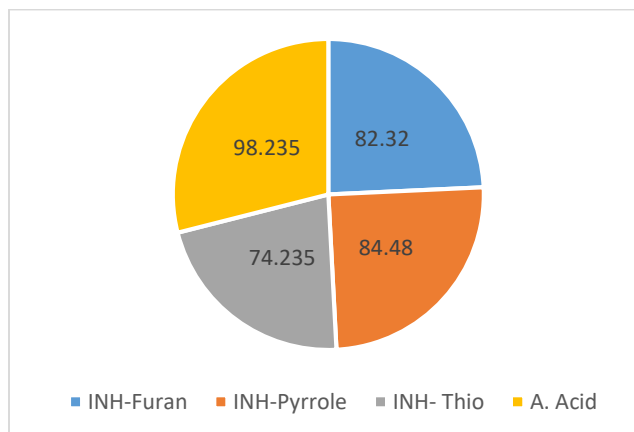


**Figure 12:** Total antioxidant capacity of INH-Furan, INH-Pyrrole, INH-Thio and Ascorbic Acid

### 3.6 Molecular docking assay

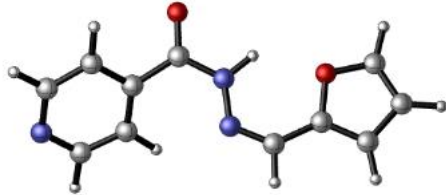
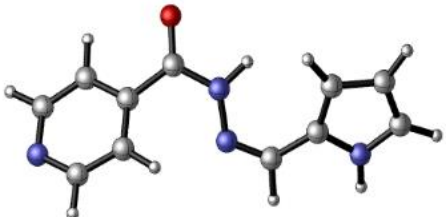
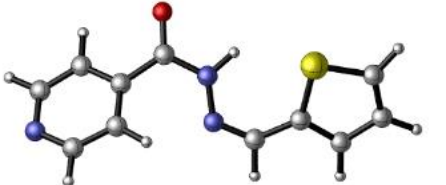
#### Binding energy of the 3POZ with the Schiff base inhibitors

The optimized structures of the Schiff base inhibitors were converted into *\*mol2* format and further used in molecular docking simulation. The names and the optimized structures are presented in Table 6. The binding energy values of the Schiff base inhibitors with the 3POZ receptor are given in Table 7. The binding energy values of the

docked inhibitors are presented in kcal/mol and the corresponding inhibition constant ( $K_i$ ) of the receptor-inhibitor in micromolar ( $\mu\text{M}$ ).

Our results suggest that INH-thiophene gave the highest BE to 3POZ, among the tested inhibitors. However, INH-Furan gave a better binding with T790M, while INH-pyrrole is more effective than other inhibitors tested on the T790M/L858R double mutant.

**Table 6:** The list of Schiff base inhibitors and their B3LYP/ 6-311+G(2d,p) level optimized molecular geometries.

No	Label	Name	Optimized Molecular Structures
1	1NH-furan	<i>N'</i> -(furan-3-ylmethylene)isonicotinohydrazide	
2	1NH-pyrrole	<i>N'</i> -((1H-pyrrol-3-yl)methylene)isonicotinohydrazide	
3	1NH-thio	<i>N'</i> -(thiophen-3-ylmethylene)isonicotinohydrazide	

**Table 7:** Binding energies and calculated inhibition constants of the Schiff bases with 3POZ and its corresponding T790M mutant and T790M/L858R double mutant

No	Inhibitor	3POZ		T790M		T790M/L858R	
		Binding Energy (kcal/mol)	$K_i$ ( $\mu$ M)	Binding Energy (kcal/mol)	$K_i$ ( $\mu$ M)	Binding Energy (kcal/mol)	$K_i$ ( $\mu$ M)
1	1NH-furan	-6.89	8.88	-6.85	9.5	-5.79	56.96
2	1NH-pyrrole	-7.27	4.72	-6.50	17.11	-5.87	50.15
3	1NH-thio	-7.51	3.14	-6.77	10.95	-5.75	61.46

The effectiveness of the inhibitors was observed to decrease from 3POZ to T790M/L858R with the BE values of -7.51, -6.85 and -5.87 kcal/mol for 3POZ, T790M and T790M/L858R. Our results in Table 7 also show that the  $K_i$  values are inverse of the

BEs of the inhibitor-receptor complexes; the higher the BE, the lower the corresponding  $K_i$  values. We therefore used the  $K_i$  values as a parameter to evaluate the effectiveness of an inhibitor. Literature evidence shows that Schiff bases are effective against EGFR

protein [52] and therefore becomes necessary to test the potency of our newly synthesized Schiff base inhibitors with the wild type and mutations of 3POZ. The inhibitors are bound to the active site of 3POZ, which is known to be located in the N-position of the A-loop, adjacent to the  $\alpha$ -helix C. The interaction diagram in Figure 1 shows the binding of 1NH-thio in the active sites of 3POZ. The important interactions that were observed are

Hydrogen bonding between the oxygen of 1NH-thio and the amino hydrogen of the Leu788 at a distance of 5.00 Å. Pi-Pi T-Shaped interaction was found between the ligand and PHE856, attractive charge interaction with ASP855. Covalent and non-covalent interactions were also observed, as can be seen in Figure 13.

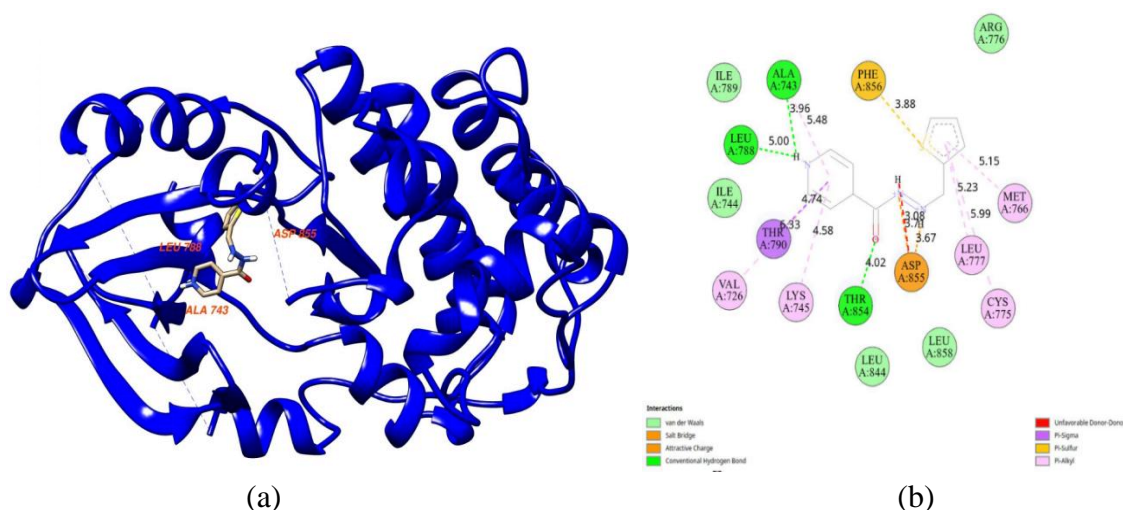
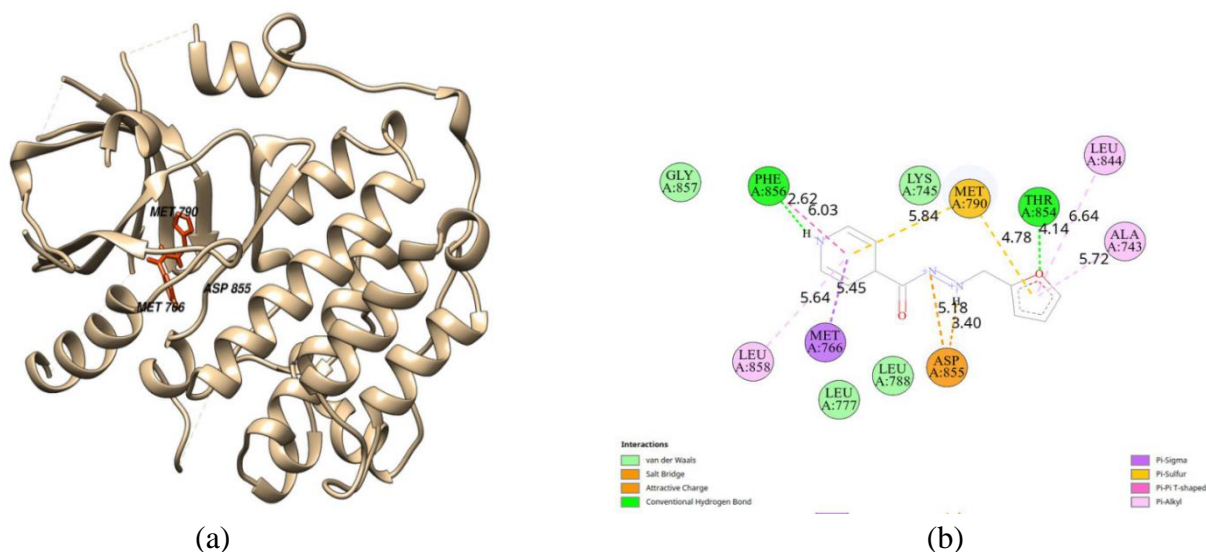


Figure 13: (a) 3D representation of the interaction of 1NH-thio in the active pocket of 3POZ, showing hydrogen bond interactions. (b) 2D representation of the interaction of 1NH-thio inhibitor with 3POZ showing various covalent bonds such as Pi-Pi T-shaped interaction and salt bridge.

### 3.7 Binding energy of the Schiff base inhibitors with the T790M mutant protein

Table 7 also shows the BE values of the tested inhibitors with the T790M mutant. The BE values are in the range -6.85 to -6.50 kcal/mol. They are lower than the BE with the wild type 3POZ, except that 1NH-furan is -6.89 kcal/mol in the wild type, which is highly comparable with the T790M mutant, with a value of -6.85 kcal/mol. Some of the

important ionic interactions of 1NH-pyrrole, such as Pi-Anion and attractive interactions were observed with ASP855. Other interactions including salt bridge and Pi-Sulphur interaction were noticed with ASP855 and MET790 respectively. The interaction diagram showing all the observed interactions of 1NH-furan with the amino acid residues of T70M are displayed in Figure 14.



**Figure 14:** (a) 3D representation of the interaction of 1NH-furan in the active pocket of T790M mutant protein. (b) 2D representation of the interaction of 1NH-furan inhibitor with T790M showing various covalent bonds such as Pi-Pi T-shaped interaction and salt bridge.

### 3.8 Binding energy of Schiff Base inhibitors with the T790M/L858R mutant

The BE values for the T790M/L858R-ligand complexes are given in Table 7. The BE values are in the range -5.87 and -5.75 kcal/mol. These values are highly comparable, indicating a similar mode of interaction of the inhibitors with the residues. Their corresponding  $K_i$  show significant variations and show low binding interaction compared to the 3POZ wild type. This is an indication that the mutation of the T790 to M790 and then L858 to R858 impacted greatly on the functionality of the protein.

The mutation further impacted greatly on the mode of interaction of the amino acid residues at the active site. The interaction diagram showing all the observed interactions of 1NH-pyrrole with the amino acid residues of T790M/L858R mutant are displayed in Figure 15. Hydrogen bonding interaction was observed with ALA1013, VAL774, LYS852, ARG776 and VAL769. The active site residues involved in the covalent interaction include CYS775, ASN771, ASP770, and ASP1014.

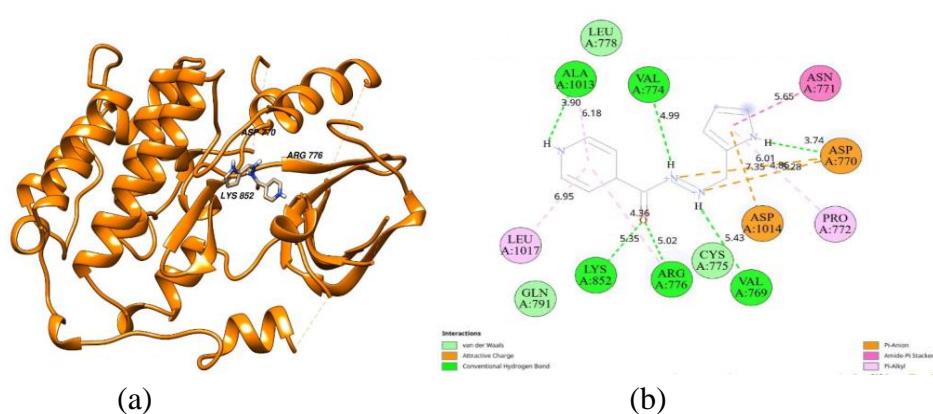


**Figure 15:** (a) The T790M/L858R mutant with 1NH-pyrrole at the active site. (b) 2D representation of the interaction of 1NH-pyrrole

#### 4.0 Conclusion

Three Schiff bases namely N'-(furan-2-ylmethylene)Ki = 50.15  $\mu$ M) showed better binding to the isonicotinohydrazide, (INH-Furan), N'-(1H-pyrrol-T790M and T790M/L858R mutants, 2-yl)methylene) isonicotinohydrazide (INH-respectively. The observed decrease in the BE Pyrrole), N'-(thiophen-2-ylmethylene) isonicotino hydrazide (INH-Thio) have been successfully synthesized. These test samples possessed good antioxidant activities comparable to the reference/standard drug, ascorbic acid thus, suggesting their possible use as supportive adjunct in the management of diseases caused by oxidative stress disorder and preservatives in food industry. However, this is subject to toxicological profile. The molecular docking results show that the Schiff bases under study demonstrate inhibitory potential against EGFR and its resistant mutant types. From the results, 1NH-thio binds (BE = -7.51 kcal/mol, Ki = 3.14  $\mu$ M) best with 3POZ wild type receptor but 1NH-furan (BE = -6.85 kcal/mol, Ki = 9.5  $\mu$ M)

and 1NH-pyrrole pyrrole (BE = -5.87 kcal/mol, Ki = 50.15  $\mu$ M) showed better binding to the isonicotinohydrazide, (INH-Furan), N'-(1H-pyrrol-T790M and T790M/L858R mutants, 2-yl)methylene) isonicotinohydrazide (INH-respectively. The observed decrease in the BE values from the 3POZ wild type receptor indicates the structural impact of resistance mutations on the Schiff base binding. The synthesized Schiff bases demonstrated significant antioxidant activity and promising inhibitory potential against EGFR wild type and resistant mutants, highlighting their potential as multifunctional therapeutic candidates.

#### Declaration of Competing Interest

The authors declare that there is no conflict of interest regarding the publication of this research paper.

#### References

1. Pruteanu, L. L., Bailey, D. S., Grădinaru, A. C., & Jäntschi, L. (2023). The biochemistry and effectiveness of antioxidants in food, fruits, and marine algae. *Antioxidants*, 12(4), 860.
2. Chaiprasongsuk, A.; & Panich, U. (2022). Role of Phytochemicals in Skin Photoprotection via Regulation of Nrf2. *Front. Pharmacol.* 13, 823-881.
3. Maandi, S. C., Maandi, M. T., Patel, A., Manville, R. W., & Mabley, J. G. (2022). Divergent effects of HIV reverse transcriptase inhibitors on pancreatic beta-cell function and survival: Potential role of oxidative stress and mitochondrial dysfunction. *Life sciences*, 294, 120329.
4. Karekar, P.; Jensen, H.N.; Russart, K.L.G.; Ponnalagu, D.; Seeley, S.; Sanghvi, S.; Smith, S.A.; Pyter, L.M.;

- Singh, H.; Gururaja, R.S. Tumor-Induced Cardiac Dysfunction: A Potential Role of ROS. *Antioxidants* 10, 1299
5. Hussain, T., Murtaza, G., Metwally, E., Kalhor, D. H., Kalhor, M. S., Rahu, B. A., & Tan, B. (2021). The role of oxidative stress and antioxidant balance in pregnancy. *Mediators of Inflammation*, 2021(1), 9962860.
  6. Cheung, E.C.; & Vousden, K.H. The role of ROS in tumour development and progression. *Nat.Rev. Cancer*, 22, 280-297.
  7. Chen, L., Chen, Y., Ding, W., Zhan, T., Zhu, J., Zhang, L., & Wang, Y. (2022). Oxidative stress-induced TRPV2 expression increase is involved in diabetic cataracts and apoptosis of lens epithelial cells in a high-glucose environment. *Cells*, 11(7), 1196.
  8. Raczuk, E., Dmochowska, B., Samaszko-Fiertek, J., & J. Madaj, J. (2022). 787 Different Schiff bases-Structure, importance and classification *Molecules*, 27, 787.
  9. Qin, W.; Long, S.; Panunzio, M.; & Biondi, S. (2013). Schiff bases: A short survey on an evergreen chemistry, *Molecules*, 18(10), 12264-89.
  10. Ibrahim, M.; Khan, A.; Ikram, M.; Rehman, S.; Shah, M.; Nabi, H.U.; Ahuchaogu, A.A. (2017). In vitro antioxidant properties of novel Schiff base complexes. *Asian J. Chem Sci.* 2, 32244
  11. Sayed, S. S., Dawood, S., Ibrahim, K., Sajjad, A., Umar, A. and Atiq R. 2020. Synthesis and Antioxidant Activities of Schiff Bases and Their Complexes: An Updated Review, *Biointerface Research in Applied Chemistry*, 10(6), 6936 – 6963.
  12. Zhang, Y.; Zou, B.; Chen, Z.; Pan, Y.; Wang, H.; Liang, H.; Yi, X. Synthesis and antioxidant activities of novel 4-Schiff base-7-benzyloxy-coumarin derivatives. *Bioorg. Med. Chem. Lett.* 21, 6811-6815.
  13. Bhagwa,t V., Digambar, K., & Avinash S. (2022). Synthesis, spectral studies, antioxidant and antibacterial evaluation of aromatic nitro and halogenated tetradentate Schiff bases. *Heliyon*, 8, <https://doi.org/10.1016/j.heliyon.2022.e09650>
  14. Aytac, S., Gundogdu, O., Bingol, Z., & Gulcin, İ. (2023). Synthesis of Schiff Bases Containing Phenol Rings and Investigation of Their Antioxidant Capacity, Anticholinesterase, Butyrylcholinesterase, and Carbonic Anhydrase Inhibition Properties. *Pharmaceutics*, 15(3), 779. <https://doi.org/10.3390/pharmaceutics15030779>
  15. El-Hussieny, M., El-Sayed,N. F., Ewies, E. F., Mansour, S. T., Aboulthana, W. M., Hussien, A. G., Al-Ashmawy, A. K. A. (2026). Iron(III) triflate, a new efficient catalyst for the synthesis of new bis (oxy)-bis (phenylene)-ethane-Schiff bases: In vitro antioxidant, anti-inflammatory,  $\alpha$ -Amylase,  $\alpha$ -Glucosidase biochemical screening, and in silico study, *Journal of Molecular Structure*, 1349(2), 143627, <https://doi.org/10.1016/j.molstruc.2025.143627>
  16. Venkatarao, Y., Sayed, Y., Bakrudeen, A.,Ahmed, A., Pandian,R., & Parthiban,P. (2026). Synthesis, spectral, crystal, docking, antioxidant, and anticancer studies of pyrazole Schiff bases, *Journal of Molecular Structure*, 1354,144863
  17. Joseyphus, R. S., & Nair, M. S.(2008). Antibacterial and Antifungal Studies on Some Schiff Base Complexes of Zinc(II). *Mycobiology*, 36(2):93-8.
  18. Kaushik, S., Paliwal, S. K., Iyer, M. R., & Patil, V. M.(2023). Promising Schiff bases

- in antiviral drug design and discovery. *Med Chem Res.*, 32(6):1063-1076.
19. Catalano, A.; Iacopetta, D.; Pellegrino, M.; Aquaro, S.; Franchini, C.; & Sinicropi, M.S. Diarylureas: Repositioning from Antitumor to Antimicrobials or Multi-Target Agents against New Pandemics. *Antibiotics*, 10, 92.
  20. Chen, S.; Liu, X.; Ge, X.; Wang, Q.; Xie, Y.; Hao, Y.; Zhang, Y.; Zhang, L.; Shang, W.; & Liu, Z. Lysosome-targeted iridium(III) compounds with pyridine-triphenylamine Schiff base ligands: Syntheses, antitumor applications and mechanisms. *Inorg.Chem. Front.* 7, 91-100
  21. Lacopetta, D., Ceramella, J., Catalano, A., Saturnino, C., Bonomo, M. G., Franchini, C., & Sinicropi, M. S. (2021). Schiff Bases-Interesting Scaffolds with promising Antitumoral properties, *Appl. Sci.*, 11, 1877
  22. Sandhu, Q-U-A., Pervaiz, M., Majid, A., Younas, U., Saeed, Z., Ashraf, A. (2023). Review: Schiff base metal complexes as anti-inflammatory agents, *J. coord. Chem.*, 1094-1118.
  23. Rana, M. S., Rayhan, N. M., Emon, M. S. H., Islam, M. T., Rathry, K., Hasan, M. M., Md. Mansur, M. I., Srijon, B. C., Islam, M. S., Ray, A., Rakib, M. A., Islam, A., Kudrat-E-Zahan, M., Md. Faruk Hossen, M. F., Asraf, M. A. (2024). Antioxidant activity of Schiff base ligands using the DPPH scavenging assay: An Updated Review. *RSC Adv.* 14(45), 33094–33123.
  24. Boudiaf, H., Latelli, N., Khelifi, R., Hamadouche, S., Merzoud, L., Morell, C., Chermette, H. (2025). Investigation of free radical scavenging activities of some Isatin Schiff bases (OH versus NH). A DFT Study,, *Chemical Physics Impact*, 11, 2025, 100904.
  25. Sogabe, S., Kawakita, Y., Igaki, S., Iwata, H., Miki, H., Cary, D. R., & Ishikawa, T. (2013). Structure-based approach for the discovery of pyrrolo [3, 2-d] pyrimidine-based EGFR T790M/L858R mutant inhibitors. *ACS medicinal chemistry letters*, 4(2), 201-205.
  26. Uribe, M. L., Marrocco, I., & Yarden, Y. 2021. EGFR in cancer: Signaling mechanisms, drugs, and acquired resistance. *Cancers*, 13(11), 2748.
  27. Sousa de Almeida, M., Roshanfekar, A., Balog, S., Petri-Fink, A., & Rothen-Rutishauser, B. 2023. Cellular uptake of silica particles influences egfr signaling pathway and is affected in response to egf. *Int. J. Nanomed.*, 1047-1061.
  28. Ayati, A., Moghimi, S., Salarinejad, S., Safavi, M., Pouramiri, B., & Foroumadi, A. (2020). A review on progression of epidermal growth factor receptor (EGFR) inhibitors as an efficient approach in cancer targeted therapy. *Bioorg. Chem.*, 99, 103811.
  29. Aertgeerts, K., Skene, R., Yano, J., Sang, B. C., Zou, H., Snell, G. & Sogabe, S. 2011. Structural analysis of the mechanism of inhibition and allosteric activation of the kinase domain of HER2 protein. *J. Bio. Chem.*, 286(21), 18756-18765.
  30. Yan, X. E., Ayaz, P., Zhu, S. J., Zhao, P., Liang, L., Zhang, C. H. & Yun, C. H. 2020. Structural basis of AZD9291 selectivity for EGFR T790M. *J. med. Chem.*, 63(15), 8502-8511.
  31. Tumbrink, H. L., Heimsoeth, A., & Sos, M. L. 2021. The next tier of EGFR resistance mutations in lung cancer. *Oncogene*, 40(1), 1-11.
  32. Han, L., Zhang, X., Wang, Z., Zhang, X., Zhao, L., Fu, W. & Wang, Y. 2021. SH-1028, an irreversible third-generation

- EGFR TKI, overcomes T790M-mediated resistance in non-small cell lung cancer. *Front. Pharmacol.*, *12*, 665253.
33. Scalvini, L., Castelli, R., La Monica, S., Tiseo, M., & Alfieri, R. 2021. Fighting tertiary mutations in EGFR-driven lung-cancers: Current advances and future perspectives in medicinal chemistry. *Biochem. Pharmacol.*, *190*, 114643.
  34. Mensor, L., Menezes, F. & Leitao, G. 2001. Screening of Brazilian plant extracts for antioxidant activity by the use of DPPH free radical method, *Phytother. Res.*, *15*, 127–130.
  35. Ghasemi, K., Ghasemi, Y. & Ebrahimzadeh, M. A. 2009. Antioxidant activity, phenol and flavonoid contents of 13 Citrus specis peels and tissues. *Pak. J. Pharm. Sci.*, *22*(3), 277-281
  36. Green, L. C., Wagner, D. A., Glogowski, J., Skipper, P. L., Wishnok, J. S., Tannenbaum S. R. 1982. Analysis of nitrate, nitrite, and [15N] nitrate in biological fluids. *Anal Biochem.* *126*,131–138.
  37. Ebrahimzadeh, M. A., Nabavi, S. M., Nabavi, S. F., Bahramian, F. & Bekhradnia, A. R. 2010. Antioxidant and free radical scavenging activity of *H. officinalis* L. VAR. *angustifolius*, *V. Odorata*, *B. Hyrcana* and *C. Speciosum*. *Pak. J. Pharm. Sci.*, *23*(1), 29-34
  38. Ke, P.J., Cervantes, E. & Robles-Martinez, C. 1984. Determination of thiobarbituric acid reactive substances (TBARS) in fish tissue by an improved distillation–spectrophotometric method, *J. Sci. Food and Agric.*, *134*, 1248-1254
  39. Yen, G. C. & Chen, H. Y. 1995. Antioxidant activity of various teas extracts in relation to their antimutagenicity. *J Agric Food Chem.*, *43*, 27–32.
  40. Prieto, P.; Pineda, M. & Aguilar, M. 1999. Spectrophotometric quantitation of antioxidant capacity through the formation of a phosphomolybdenum complex: Specific application to the determination of vitamin E. *Anal. Biochem.*, *269*, 337-341.
  41. Morris, G. M.; Huey, R.; Lindstrom, W.; Sanner, M. F.; Belew, R. K.; Goodsell, D. S. & Olson, A. J. 2009. AutoDock4 and AutoDockTools4: Automated docking with selective receptor flexibility. *J. Comput. Chem.*, *30*, 2785–2791.
  42. Nguyen, N. T., Nguyen, T. H., Pham, T. N. H., Huy, N. T., Bay, M. V., Pham, M. Q. & Ngo, S. T. 2019. Autodock vina adopts more accurate binding poses but autodock4 forms better binding affinity. *J. Chem. Inf. Model.* *60*(1), 204-211.
  43. Dooley, R., Milfeld, K., Guiang, C., Pamidighantam, S. & Allen, G. 2006. From proposal to production: Lessons learned developing the computational chemistry grid cyberinfrastructure. *J. Grid Comput*, *4*, 195-208.
  44. Pettersen, E. F., Goddard, T. D., Huang, C. C., Meng, E. C., Couch, G. S., Croll, T. I., & Ferrin, T. E. 2021. UCSF ChimeraX: Structure visualization for researchers, educators, and developers. *Protein sci.*, *30*(1), 70-82.
  45. Fasina, T.M., Dueke-Eze, C. U., & FAMILONI, O. (2018). Synthesis and solvatochromic behaviour of some heterocyclic Isonicotinohydrazide Schiff bases, *Moroccan J. Chem.*, *6*(3), 504-510.
  46. Olszowy-Tomczyk, M. (2021). How to express the antioxidant properties of substances properly? *Chemical Papers.* *75*:6157–6167.

- <https://doi.org/10.1007/s11696-021-01799-1>
47. Lang, Y., Gao, N., Zang, Z., Meng, X., Lin, Y., Yang, S., Yang, Y., Jin, Z., & Li, B. (2024). Classification and antioxidant assays of polyphenols: a review, *Journal of Future Foods*, 4(3), 193-204, ISSN 2772-5669, <https://doi.org/10.1016/j.jfutfo.2023.07.002>.
  48. Gulcin, İ., & Alwasel, S. H. (2023). DPPH Radical Scavenging Assay. *Processes*, 11(8), 2248. <https://doi.org/10.3390/pr11082248>
  49. Gulcin, İ., & Alwasel, S. H. (2025). Fe<sup>3+</sup> Reducing Power as the Most Common Assay for Understanding the Biological Functions of Antioxidants. *Processes*, 13(5), 1296. <https://doi.org/10.3390/pr13051296>
  50. Can, Z., Keskin, B., Üzer, U., & Apak, R. (2022). Detection of nitric oxide radical and determination of its scavenging activity by antioxidants using spectrophotometric and spectrofluorometric methods, *Talanta*, 238, (1), 122993, ISSN 0039-9140, <https://doi.org/10.1016/j.talanta.2021.122993>.
  51. Brainina, K., Stozhko, N., & Vidrevich, M. (2019) Antioxidants: Terminology, Methods, and Future Considerations. *Antioxidants* 8:297–304.
  52. Othman, D. I., Hamdi, A., Elhousseiny, W. M., El-Azab, A. S., Bakheit, A. H., Hefnawy, M., & Alaa, A. M. 2023. Synthesis of novel spirochromane incorporating Schiff's bases, potential antiproliferative activity, and dual EGFR/HER2 inhibition: Cell cycle analysis and in silico study. *Saudi Pharm. J.*, 31(11), 101803.